

Electromechanical switch based on pentaheptite nanotubes

I. Milošević,^{1,*} Z. Popović,¹ G. Volonakis,² S. Logothetidis,² and M. Damnjanović^{1,†}

¹NanoLab, Faculty of Physics, University of Belgrade, P.O. Box 368, 11001 Belgrade, Serbia

²Department of Physics, Aristotle University of Thessaloniki, GR-54124 Thessaloniki, Greece

(Received 8 July 2007; published 10 September 2007)

Full symmetry of the nanotubes rolled up from pentaheptite carbon lattices along an arbitrary chiral vector is determined, and symmetry preserving relaxation of a large number of the simply rolled-up tubular structures is performed in order to assess stability and conducting properties of the pentaheptite nanotubes relative to the classical graphitic nanotubes. Density functional tight binding calculations are performed by full-symmetry implemented POLSYM code. The vast majority of pentaheptite nanotubes is found to be metallic having considerably higher electronic density of states at Fermi level than their metallic conventional counterparts. Pathway for synthesis of certain types of pentaheptite nanotubes directly from the conventional hexagonal nanotubes by putting them under uniaxial tension is proposed. Release of the strain goes through formation of double pentagon-heptagon pairs. The findings promise application as mechanically induced electrical switches.

DOI: 10.1103/PhysRevB.76.115406

PACS number(s): 85.65.+h, 61.48.+c, 71.20.Tx, 72.80.Rj

I. INTRODUCTION

Intensive research of various carbon based nanostructures, in particular, nanotubes,¹ is to a large extent motivated by possible technological applications.² Even more striking effects may be obtained when different structures and properties are combined. Theoretically, graphene can be converted into carbon planar pentaheptite sheet by simultaneous application of the Stone-Wales bond rotation,^{3,4} which transforms four adjacent graphene hexagons into two pentagon-heptagon pairs. However, synthesis of pentaheptite modifications of the graphite sheet still remains challenging and thus far pentagon-heptagon tiling has been realized only in boron nets⁵ of YCrB₄ and ThMoB₄. These ternary borides form face-regular (1,3)-pentaheptite structures where each pentagon has one pentagonal neighbor and each heptagon has three heptagonal neighbors. Symmetry of their lattices is described by hexagonal (ThMoB₄) and rectangular (YCrB₄) diperiodic groups.^{6,7}

In this paper, we present theoretical study of the pentaheptite nanotubes, 57NTs (5 and 7 reflecting the two ring types), obtained by rolling up hexagonal and rectangular (1,3)-pentaheptite carbon lattices along an arbitrary chiral vector. We determine the symmetry of the 57NTs and perform symmetry preserving relaxation of a large number of simply rolled-up tubular structures in order to assess the stability and conducting properties of the 57NTs. Density functional tight binding (DFTB) calculations⁹ are performed by full-symmetry implemented POLSYM code.¹⁰ Pentaheptite tubes are found to be less stable than their conventional counterparts but more stable than the pentaheptite carbon sheet. We propose a pathway for synthesis of certain types of pentaheptite nanotubes directly from the conventional nanotubes by putting them under uniaxial tension. Release of the strain goes through formation of double pentagon-heptagon pairs.¹¹

II. SYMMETRY

Hexagonal and rectangular planar carbon (1,3)-pentaheptite nets are given in Fig. 1. Unit cells of the both

structures contain eight carbon atoms. However, in our calculations, instead of the unit cell, the *symcell* is used; this is the minimal set of atoms from which, by applying *all* symmetry transformations, the whole structure is generated.¹²

Doubled graphite lattice constant $a_0=2.461$ Å becomes the constant of the hexagonal pentaheptite tiling and the unit vectors are $\mathbf{a}_1=2a_0\mathbf{e}_x$ and $\mathbf{a}_2=a_0(\mathbf{e}_x+\sqrt{3}\mathbf{e}_y)$. Symmetry is described by the hexagonal diperiodic group DG47 (*cmm*), and this is the only (1,3)-pentaheptite group which contains a reflection.^{6,7} As the net is composed of three orbits⁸ (one general and the other two on the mirror planes), the *symcell* contains three atoms.

Vectors $\mathbf{a}_1=a_0(\mathbf{e}_x-\sqrt{3}\mathbf{e}_y)$ and $\mathbf{a}_2=a_0(\frac{3}{2}\mathbf{e}_x+\frac{\sqrt{3}}{2}\mathbf{e}_y)$ are the basis of the rectangular lattice. Its symmetry is described by the diperiodic group^{6,7} DG6 (*pgg*). The lattice with four orbits is generated by the *symcell* comprised of four carbon atoms.

Hexagonal and rectangular pentaheptite nanotubes (H57NTs and R57NTs) are obtained by rolling up hexagonal and rectangular planar carbon (1,3)-pentaheptite nets along a chiral vector $\mathbf{c}=n_1\mathbf{a}_1+n_2\mathbf{a}_2$, which then becomes a circumference of the (n_1, n_2) tube (Fig. 2). Chiral angle is also de-

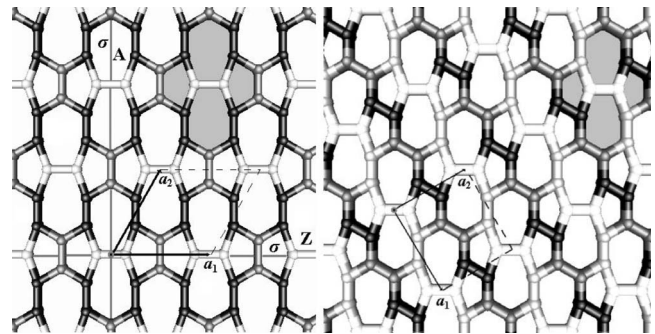


FIG. 1. Hexagonal (left) and rectangular (right) pentaheptite layers with unit vectors and elementary cells (dashed). Double pentagon-heptagon motifs are shaded. Orbits are distinguished by gray tones. For hexagonal tiling, zigzag (Z) and armchair (A) directions are along the symmetry planes σ denoted by gray lines. Gray circle is the C_2 axis (U axis of NTs).

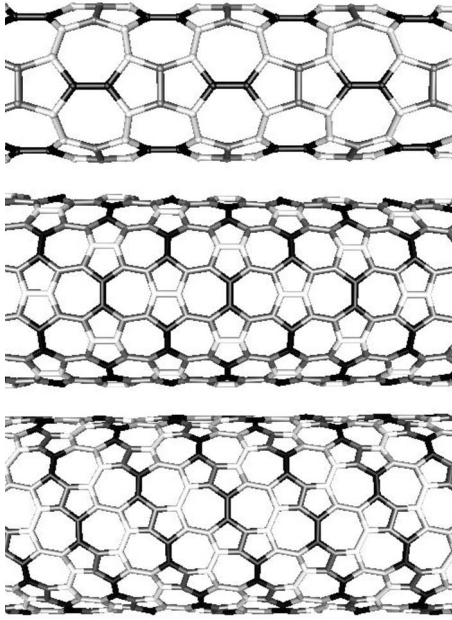


FIG. 2. Pentaheptite carbon nanotubes: armchair $(-3,6)$ and zigzag $(7,0)$ H57NTs and chiral $(4,8)$ R57NT (from top to bottom). Orbits are distinguished by gray tones.

fined in a usual way: $\theta = \angle(\mathbf{a}_1, \mathbf{c})$ and its range is $[0, \pi/2]$ for H57NTs and $[0, \pi]$ for R57NTs. If inverse Stone-Wales transformation is applied on all pentagon-heptagon double pairs of a 57NT, a conventional nanotube is regained. To each 57NT corresponds one conventional nanotube and we call it the *generic nanotube*. Namely, if (n_1, n_2) are chiral indices of a H57NT, its generic (conventional) nanotube is $(2n_1, 2n_2)$ (or the equivalent one with $\theta \leq 30^\circ$). Similarly, $(2n_1 + n_2, -2n_1 + n_2)$ is the generic nanotube of the (n_1, n_2) R57NT.

Generally, symmetry of the (n_1, n_2) 57NT is described by a line group of the fifth family, which is a product of screw-axis group $T_q^r(a)$, rotational group C_n , $n = \text{GCD}(n_1, n_2)$, and D_1 group, generated by $(C_q^r | an/q)$ (simultaneous rotation for $2\pi r/q$ around the tube axis and translation for an/q along the same axis), C_n (rotation for $2\pi/n$ around the tube axis), and rotation for π around a horizontal axis, the so-called U axis.

The group parameters q , r , and n for H57NTs are the same as for the conventional nanotubes,¹³ and only the period a is doubled:

$$n = \text{GCD}(n_1, n_2), \quad q = 2 \frac{n_1^2 + n_1 n_2 + n_2^2}{n\mathcal{R}}, \quad a = \frac{\sqrt{3}D\pi}{n\mathcal{R}}, \quad (1)$$

where $D = \sqrt{2nq\mathcal{R}a_0}/\pi$ is the tube diameter, $\mathcal{R} = \text{GCD}(2n_1 + n_2, n_1 + 2n_2)/n$, while r is a more complicated number theoretical function.

For R57NTs, the line group parameters are¹⁴

$$q = \frac{4n_1^2 + 3n_2^2}{n\mathcal{R}}, \quad a = \frac{\sqrt{12}D\pi}{n\mathcal{R}}. \quad (2)$$

Here, the tube diameter is $D = \sqrt{nq\mathcal{R}a_0}/\pi$ and $\mathcal{R} = \text{GCD}(3, n_1/n)\text{GCD}(4, n_2/n)$.

Relative to the translational period of a generic nanotube, the period of a corresponding R57NT quadruples or doubles or remains the same.

While all R57NTs are chiral, H57NTs can either be chiral ($0 < |n_1| < n_2, 0^\circ < \theta < 90^\circ$) or achiral (with identical left and right isomers), i.e., of the zigzag ($n_2 = 0, \theta = 0^\circ$) and of the armchair ($n_2 = -2n_1, \theta = 90^\circ$) type. Apart from the fifth family line group symmetry, the achiral tubes have mirror invariance and their full symmetry is thus described by the line groups belonging to the 13th family:

$$L^{(13)} = T_q^r(a)D_{nh}, \quad \text{achiral H57NTs}, \quad (3)$$

$$L^{(5)} = T_q^r(a)D_n, \quad \text{chiral 57NTs}. \quad (4)$$

III. STRAIN

Simply rolled-up pentaheptite layer configuration is not energetically the most favorable, as the curvature induces an additional tension with respect to the layer. Therefore, in order to find the configurations with the lowest energy, the symmetry preserving density functional⁹ relaxation is applied: only the coordinates of the symcell atoms are varied, as according to the topological theorem of Abud and Sartori,¹⁵ the extremes of the invariant functions are on the manifolds with maximal symmetry. In contrast to the conventional carbon nanotubes, which are generated from a single atom by action of the full-symmetry group,¹³ chiral 57NTs are generated from four and achiral H57NTs from three atoms. Thus, 13 (or ten in the case of achiral H57NTs) parameters are optimized, as apart from the unit cell length, only the coordinates of the symcell atoms are varied.

Quite generally, the optimized 57NTs have slightly corrugated tubular structure, as the diameters of the different orbits are independently varied. Further, relaxed structures have more regular pentagons and heptagons. Accordingly, optimization leads to chirality dependent change of period accompanied by the opposite change in average diameter. For H57NTs, value of d (average diameter of the relaxed vs simply rolled-up 57NT) decreases, approaching zero at $\theta_c \approx \pi/3$, where from the relaxed structures become more narrow (relative to the unrelaxed ones). In particular, relaxed zigzag tubes are $\sim 20\%$ thicker, while optimization procedure diminishes the diameter of the armchair H57NTs for $\sim 10\%$. In the case of the R57NTs, relative change of the diameter increases with the chiral angle. These oscillations of the d value of 57NTs with the similar diameter but different chiral angle are attributed to the curvature effects.

In Fig. 3, the calculated diameter dependencies of the curvature strain energies, i.e., the differences of the total energies (per atom) between the 57NTs and the corresponding pentaheptite layer, are shown. The calculated strain energies of the 57NTs follow roughly $1/D^2$ behavior as in conventional carbon nanotubes.¹⁶

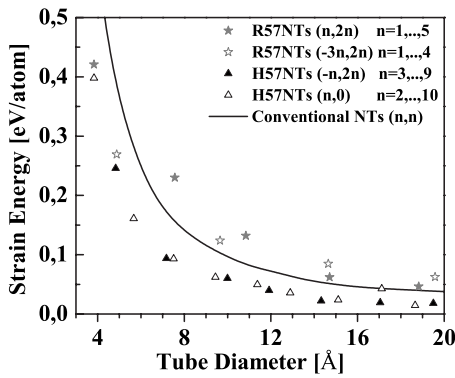


FIG. 3. Curvature induced strain energy of 57NTs as a function of the tube diameter. Strain of graphitic armchair nanotubes is shown for comparison.

Our calculations show that the curvature strain energy of the achiral H57NTs is lower than the strain energy of the conventional graphitic nanotubes, which is in accordance with the calculations of Terrones *et al.*,¹⁷ where the strain energy of the zigzag H57NTs is presented. We find the energies of the relaxed H57 and R57 sheets to be, respectively, 297 and 329 meV/atom above that of graphene. The former value is a bit less than the estimations reported in Refs. 4 and 17, while the latter has not been reported yet. Strain energy of the R57NTs is slightly larger than the strain of the graphitic and hexagonal pentaheptite nanotubes. Nevertheless, R57NTs should also be feasible as their strain is just a few meV larger than the strain of the graphitic nanotubes with the same diameter.

IV. CONDUCTING PROPERTIES

Figure 4 shows that vast majority of 57NTs has considerably larger electronic density of states (DOS) at the Fermi level than their graphitic armchair counterparts. This is due to the band topology of 57NTs, which is characterized by several subband crossings at the Fermi level, Fig. 5. However, this is not the rule: Some of the 57NTs, although generated from conventional (n,n) tubes, turn out to be either narrow or moderate band gap semiconductors (see Table I).

Calculations of the electronic band structure of the defective (n,n) tubes¹⁸ showed that DOS at Fermi level increases

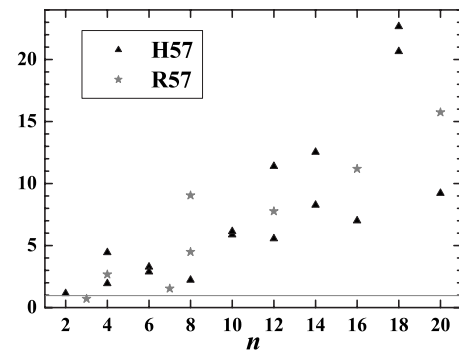


FIG. 4. Rate of the DOS at the Fermi level of the 57NTs and their (n,n) graphitic counterparts.

with the concentration of bond-rotation defects. Our calculations reveal that direct extrapolation of the results obtained for the defective nanotubes is not plausible. Namely, unlike the case of nanotubes with 2% or 3% of bond-rotation defects, for the 57NTs, perturbative approach (i.e., analysis of the evolution of the electronic structure of a graphitic sheet upon introduction of the defects) is not applicable. Besides, only armchair nanotubes which have even chiral index can be converted, by means of Stone-Wales C-C bond rotations, into H57NTs, while graphitic $(2k+1, 2k+1)$ tubes can be converted into $(0, 2k+1)$ R57NTs. In particular, $(0,5)$ and $(0,9)$ R57NTs are narrow band gap semiconductors (Table I).

Quantum and classical simulations¹¹ show that strain release in carbon nanotubes under uniaxial tension larger than 5% goes through reversible formation of topological defects, the simplest of which is the Stone-Wales rotation of a C-C bond. Plausible conjecture is that further increasing of the strain could yield onset of Stone-Wales deformations and ultimate crossover from a graphitic to a pentaheptite nanotube, especially if the activation barrier for a Stone-Wales bond rotation within the stretched generic classical nanotube is not too high.¹⁹⁻²¹

In Fig. 6, change of the total energy (at 0 K) of the $(10,10)$ graphitic nanotube under uniaxial strain is shown. Our calculations predict that stretched generic $(10,10)$ tube for more than 10.8% becomes less energetically favorable than hexagonal pentaheptite $(-5,10)$ nanotube. Such an elongation falls well below the experimental values of the breaking strain level.²²

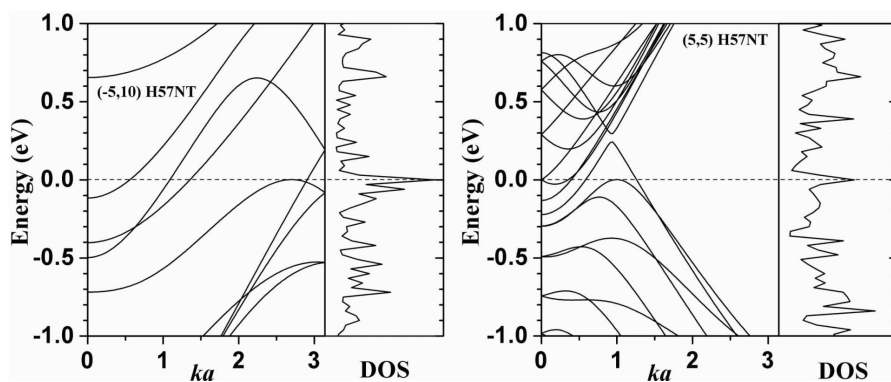


FIG. 5. Electronic band structure and density of states in the Fermi level region of the hexagonal pentaheptite nanotubes $(-5,10)$ and $(5,5)$. For both tubes, the generic graphitic nanotube is $(10,10)$.

TABLE I. Gap sizes of the nonmetallic R57 and H57 NTs, which can be converted (by means of Stone-Wales C-C bond rotations) from the metallic (n, n) graphitic tubes.

n	R57NT	Gap size (eV)	H57NT	Gap size (eV)
2	(0,2)	0.290	(-1, 2)	1.228
4	(3,2)	0.123		
	(0,4)	0.318		
5	(0,5)	0.307		
6	(0,6)	0.111		
8	(0,8)	0.167	(4,4)	1.283
9	(0,9)	0.304		
10	(0,10)	0.363		
12	(9,6)	0.294		
16	(12,8)	0.772	(8,8)	0.777
20			(10,10)	0.200

Recall that the configuration of $(-5, 10)$ H57NT is generated by applying Stone-Wales transformations on all diamond shaped primitive cells of hexagons of the classical $(10,10)$ nanotube. The other two 57NTs for which $(10,10)$ is also generic, i.e., $(0,10)$ R57NT and $(5,5)$ H57NT, become energetically preferable when uniaxial strain exceeds 15% and 20%, thus approaching the failure strain of the armchair carbon nanotubes.¹⁹

V. CONCLUSION

We have found unique relation between the chiral vector indices of the hexagonal and rectangular pentaheptite allotropic modifications of the graphitic nanotubes and their full symmetry groups. The latter we have used to perform symmetry preserving relaxation of the simply rolled-up carbon pentaheptite sheets. Electronic band structure and curvature induced strain energy are calculated by means of DFTB within full symmetry implemented POLSYM code. Hexagonal 57NTs are found to be more stable than the R57NTs. In particular, the calculated strain energy of the armchair and zigzag H57NTs is lower than the strain energy of conventional nanotubes with similar diameter. Achiral H57NTs are metallic, irrespective of the conducting properties of their graphitic counterparts. Electronic DOS at the Fermi level of the $(n,0)$ and $(-n,2n)$ H57NTs is, at last, several times larger than DOS of the classical armchair nanotubes. However, neither all H57NTs nor all R57NTs are metallic, not even if their generic tubes are of the armchair type.

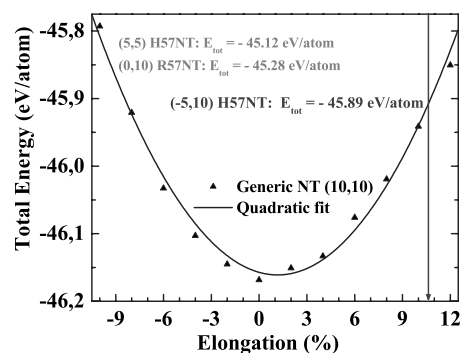


FIG. 6. Total energy of the graphitic $(10,10)$ tube under uniaxial strain. Values of the total energies of the 57NTs for which $(10,10)$ is a generic tube are given. Arrow indicates threshold extension of classical nanotube, for which its energy reaches the total energy of relaxed $(-5, 10)$ H57NT. The other two 57NTs are contracted with respect to the generic nanotube.

Total energy calculations indicate that spontaneous growth of 57NTs is not likely as graphitic nanotubes are energetically preferable. However, difference in total energy is not large: In the case of the $(-5, 10)$ H57NT and its generic $(10,10)$ tube, $\Delta E_{\text{tot}} \approx 250$ meV. Hence, it is plausible to induce the allotropic transition by an external field. Namely, if within the plastic deformation, which can be controlled by the direction and strength of the strain applied, the parameters of the generic nanotube (nearly) matches the parameters of the corresponding most favorable pentaheptite allotrope, the activation barrier is expected to be accessible.

Numerical simulations have shown that under tensile strain, the total energy of the graphitic nanotubes increases, approaching the energy of the pentaheptite counterparts. Besides, period and diameter of the classical tubes change simultaneously, matching the values of the corresponding relaxed achiral pentaheptite tubular structures. Hence, allotropic transition can be mechanically induced and, depending on the conducting properties of the graphitic nanotube, it is either (moderate or narrow band gap) semiconductor—metal or semimetal—metal phase transition. The findings promise application as mechanically induced electrical switches.

ACKNOWLEDGMENTS

We thank G. Seifert, TU Dresden, for DFTB matrix elements data. This work is supported by the Serbian Ministry of Science (Project No. ON141017) and European Union (FP6 INCO-WBC 026303 project).

*ivag@rcub.bg.ac.yu

†URL: <http://nanolab.ff.bg.ac.yu>

¹S. Reich, C. Thomsen, and J. Maultzsch, *Carbon Nanotubes: Basic Concepts and Physical Properties* (Wiley-VCH, Weinheim, 2004).

²*Applied Physics of Nanotubes: Fundamentals of Theory, Optics and Transport Devices*, edited by S. V. Rotkin and S. Subramoney (Springer-Verlag, Berlin, 2005).

³A. J. Stone and D. J. Wales, *Chem. Phys. Lett.* **128**, 501 (1986).

⁴V. H. Crespi, L. X. Benedict, M. L. Cohen, and S. G. Louie, *Phys.*

- Rev. B **53**, R13303 (1996).
- ⁵M. O’Keeffe and B. G. Hyde, *Crystal Structures* (Mineralogical Society of America, Washington, DC, 1996).
- ⁶Elisabeth Wood, Bell System Monograph No. 4680, 1964.
- ⁷M. Deza, P. W. Fowler, M. Shtogrin, and K. Vietze, Chem. Phys. Lett. **40**, 1325 (2000).
- ⁸*Orbit* of a system is a subsystem elements of which are connected by a symmetry transformation.
- ⁹D. Porezag, T. Frauenheim, T. Köhler, G. Seifert, and R. Kaschner, Phys. Rev. B **51**, 12947 (1995).
- ¹⁰I. Milošević, A. Damjanović, and M. Damnjanović, in *Quantum Mechanical Simulation Methods in Studying Biological Systems*, Les Editions de Physique, Les Ulis, edited by D. Bicout and M. Field (Springer-Verlag, Berlin, 1996), Chap. XIV, pp. 295–311.
- ¹¹M. Buongiorno Nardelli, B. I. Yakobson, and J. Bernholc, Phys. Rev. B **57**, R4277 (1998).
- ¹²M. Damnjanović, I. Milošević, E. Dobardžić, T. Vuković, and B. Nikolić, in *Applied Physics of Nanotubes; Fundamentals of Theory, Optics and Transport Devices* (Ref. 2), Chap. 2, pp. 41–88.
- ¹³M. Damnjanović, I. Milošević, T. Vuković, and R. Sredanović, Phys. Rev. B **60**, 2728 (1999).
- ¹⁴M. Damnjanović, B. Nikolić, and I. Milošević, Phys. Rev. B **75**, 033403 (2007).
- ¹⁵M. Abud and G. Sartori, Ann. Phys. (N.Y.) **150**, 307 (1983).
- ¹⁶E. Hernández, C. Goze, P. Bernier, and A. Rubio, Phys. Rev. Lett. **80**, 4502 (1998).
- ¹⁷H. Terrones, M. Terrones, E. Hernández, N. Grobert, J.-C. Charlier, and P. M. Ajayan, Phys. Rev. Lett. **84**, 1716 (2000).
- ¹⁸V. H. Crespi, M. L. Cohen, and A. Rubio, Phys. Rev. Lett. **79**, 2093 (1997).
- ¹⁹T. Dumitrica, M. Hua, and B. I. Yakobson, Proc. Natl. Acad. Sci. U.S.A. **103**, 6109 (2006).
- ²⁰B. I. Yakobson, Appl. Phys. Lett. **72**, 918 (1998).
- ²¹P. Zhang, P. E. Lammert, and V. H. Crespi, Phys. Rev. Lett. **81**, 5346 (1998).
- ²²M. Yu, O. Lourie, M. Dyer, K. Moloni, T. Kelly, and R. S. Ruoff, Science **287**, 637 (2000); M.-F. Yu, B. S. Files, S. Arepalli, and R. S. Ruoff, Phys. Rev. Lett. **84**, 5552 (2000).